Editors' Suggestion | Featured in Physics

Femtosecond Rotational Dynamics of D_2 Molecules in Superfluid Helium Nanodroplets

Junjie Qiang,[1,*] Lianrong Zhou,[1,*] Peifen Lu,[1,†] Kang Lin,[1] Yongzhe Ma,[1] Shengzhe Pan,[1] Chenxu Lu,[1] Wenyu Jiang,[1] Fenghao Sun,[1] Wenbin Zhang,[1] Hui Li,[1] Xiaochun Gong,[1] Ilya Sh. Averbukh,[2] Yehiam Prior,[1,2] Constant A. Schouder,[3] Henrik Stapelfeldt,[3,‡] Igor N. Cherepanov,[4] Mikhail Lemeshko,[4] Wolfgang Jäger,[5] and Jian Wu[1,6,7,§]

[1]*State Key Laboratory of Precision Spectroscopy, East China Normal University, Shanghai 200241, China*
[2]*AMOS and Department of Chemical and Biological Physics, Weizmann Institute of Science, Rehovot 76100, Israel*
[3]*Department of Chemistry, Aarhus University, Langelandsgade 140, 8000 Aarhus C, Denmark*
[4]*Institute of Science and Technology Austria, Am Campus 1, 3400 Klosterneuburg, Austria*
[5]*Department of Chemistry, University of Alberta, Edmonton, Alberta T6G 2G2, Canada*
[6]*Collaborative Innovation Center of Extreme Optics, Shanxi University, Shanxi 030006, China*
[7]*CAS Center for Excellence in Ultra-intense Laser Science, Shanghai 201800, China*

(Received 23 January 2022; revised 7 April 2022; accepted 9 May 2022; published 16 June 2022)

Rotational dynamics of D_2 molecules inside helium nanodroplets is induced by a moderately intense femtosecond pump pulse and measured as a function of time by recording the yield of HeD^+ ions, created through strong-field dissociative ionization with a delayed femtosecond probe pulse. The yield oscillates with a period of 185 fs, reflecting field-free rotational wave packet dynamics, and the oscillation persists for more than 500 periods. Within the experimental uncertainty, the rotational constant B_{He} of the in-droplet D_2 molecule, determined by Fourier analysis, is the same as B_{gas} for an isolated D_2 molecule. Our observations show that the D_2 molecules inside helium nanodroplets essentially rotate as free D_2 molecules.

DOI: 10.1103/PhysRevLett.128.243201

Laser-induced alignment of molecules in the gas phase has been intensively studied in the last decades and used in various applications [1–4]. In particular, moderately intense femtosecond laser pulses can create rotational wave packets, i.e., coherent superpositions of field-free rotational eigenstates, leading to alignment and antialignment revivals in narrow, periodically occurring time windows. For isolated linear and symmetric top molecules, the characteristic revival structure of the time-dependent degree of alignment, explored in a large number of works, persists and does not change provided coupling of the rotational angular momentum to, e.g., the nuclear spin is negligible [5,6]. On the other hand, if the molecules are in a dense gas, collisions with other molecules or atoms will lead to a gradual dephasing of the wave packet and possibly rotational state redistribution, which manifests as a gradual disappearance of the revival structures [7–9].

Recently, alignment in the nonadiabatic regime was extended to molecules embedded in liquid helium nanodroplets [10–13]. Studies on OCS, CS_2, and I_2 molecules showed that when their rotational energy is kept well below the roton energy of the droplet [14,15], where coupling between rotation and the phonons is weak, revivals are present in the time-dependent degree of alignment traces, reflected as discrete peaks in the corresponding frequency spectra. These observations were interpreted as a consequence of the superfluidity of He droplets. Although the observed rotational dynamics differed strongly from the rotational dynamics of gas-phase molecules, a free-rotor model accounted for the experimental results [12]. It revealed that the difference is due to the smaller effective rotational constant B_{He} and the much larger centrifugal distortion constant D_{He} of the in-droplet molecules [14,15] compared to those of the gas-phase molecules, B_{gas} and D_{gas}, as well as to a distribution rather than a single value of B_{He} and D_{He}.

For OCS, CS_2, and I_2, the B_{gas}/B_{He} ratio lies between 2 and 5, an effect caused by a nonsuperfluid density of He corotating with the molecules [16]. For smaller and lighter molecules, B_{gas}/B_{He} tends toward 1, notably when $B_{gas} > 1\ cm^{-1}$. This trend, qualitatively explained as the surrounding He atoms not being able to follow the fast-rotating molecules, indicates that the rotation of small molecules inside He droplets should closely resemble that in the gas phase. However, the collected information from a large number of infrared (ir) spectroscopy studies have established that $D_{He} = 0.038 B_{He}^{1.88}$ at least up to $B_{He} = 1\ cm^{-1}$ [15]. Although it is not clear if this correlation between D_{He} and B_{He} is still valid when $B_{He} > 1\ cm^{-1}$, ir studies on methane ($B_{He} = 5.0\ cm^{-1}$) showed that D_{He} remains significantly larger than D_{gas} [17]. Such a situation will lead to rotational dynamics very different from that of gas-phase molecules. On the other hand, the quasiparticle angulon model recently predicted that in the limit of light rotors, D_{He} scales as B_{He}^{-1}, which would point toward

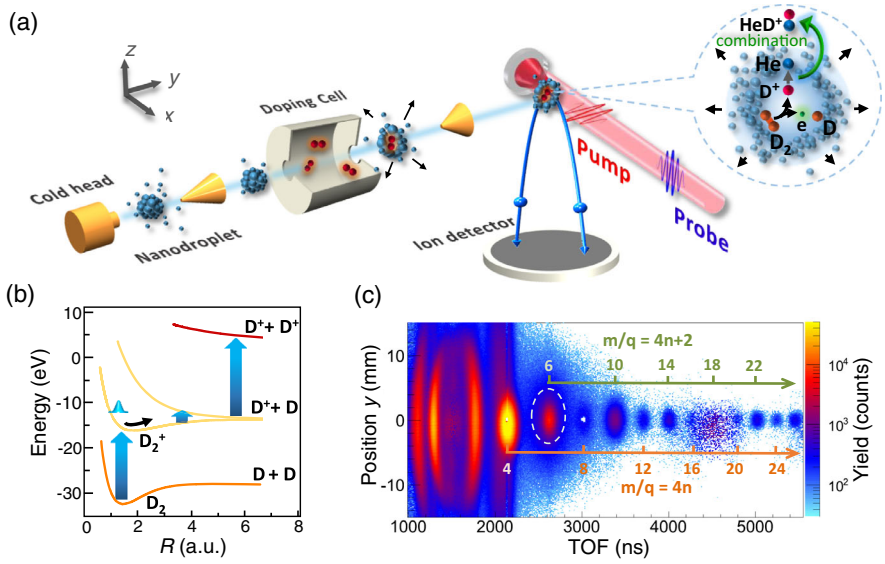

FIG. 1. (a) Schematic diagram of the experimental setup. (b) Relevant potential energy curves of D_2, D_2^+, and D_2^{2+} ($1/R$ Coulomb potential), adapted from Ref. [26]. The blue vertical arrows illustrate the $D_2(1,0)$ and $D_2(1,1)$ dissociative ionization channels; see text. (c) Measured position y-TOF spectrum of the ions produced when the probe pulse interacts with the doped He nanodroplets. The signal originating from the residual gas in the interaction chamber (e.g., H_2, H_2O, and N_2) was subtracted from the spectrum for clarity.

a gas-phase-like rotation [Ref. [18], Sec. V]. This leaves an open question: How do small and light molecules ($B_{\mathrm{gas}} \gg 1\ \mathrm{cm}^{-1}$) rotate inside superfluid He droplets? The purpose of our work is to answer this question. It is done by using a nonresonant femtosecond pulse to create rotational wave packets in D_2 molecules embedded in helium nanodroplets and measuring the rotational dynamics through timed strong-field dissociative ionization.

A schematic of the experimental setup is given in Fig. 1(a). A continuous helium nanodroplet beam was produced by expanding ^{4}He gas (99.9999%, 16.2 K, 20 bar) through a 5-μm-diameter nozzle. The droplets, estimated to contain on average 2000 He atoms [14], were doped by passing them through a 4-cm-long pickup cell with D_2 gas. Two linearly polarized pulsed laser beams were focused by a concave silver mirror ($f = 7.5$ cm) onto the doped He droplets inside a cold target recoil ion momentum spectroscopy (COLTRIMS) setup [24,25]. The pulses in the pump beam (790 nm, ~40 fs, y-polarized, 8.0×10^{13} W/cm^2) were used to induce alignment and the pulses in the probe beam (395 nm, ~30 fs, z-polarized, 2.0×10^{14} W/cm^2) were used to measure the degree of alignment.

In previous studies of laser-induced alignment of molecules in He droplets, the degree of alignment was measured by Coulomb exploding the molecules with an intense laser pulse and recording the emission directions of the fragment ions [10,27]. Fragment ions like I^+, Br^+, or S^+ from, e.g., I_2, C_6H_5Br, and CS_2 molecules, respectively, lose some of their initial directionality following the Coulomb explosion event due to scattering on He atoms as the ions move out of the droplet, but their final angular distribution can still be used to determine the degree of alignment [27,28]. For the much lighter fragment ion D^+, the influence of the He scattering on the ion trajectories is more severe, and our experiment shows that the Coulomb explosion probe method is not well suited [18]. Instead, the rotational dynamics is probed by ionizing the D_2 molecules with the probe pulse and measuring the dissociative-ionization yield because it depends on the orientation of the molecular axis relative to the polarization of the probe pulse.

The alignment-dependent dissociative-ionization process details are illustrated in Fig. 1(b). The probe pulse ionizes and dissociates the D_2 molecule via two channels: $D_2 \rightarrow D_2^+ + e \rightarrow D^+ + D + e$, denoted as $D_2(1,0)$, and $D_2 \rightarrow D_2^+ + e \rightarrow D^+ + D^+ + 2e$, denoted as $D_2(1,1)$. Both channels are sequential, and the first step is multiphoton ionization of D_2. The ionization step depends only mildly on the molecular alignment [29,30]. The subsequent step is a parallel transition between the $1s\sigma_g$ and $2p\sigma_u$ states of D_2^+ [31] before either dissociating to D^+ and D [the $D_2(1,0)$ channel] or undergoing charge-resonance-enhanced ionization [32] followed by Coulomb explosion to D^+ and D^+ [the $D_2(1,1)$ channel]. Both of these two channels occur most effectively when the molecular axis aligns along the polarization direction of the laser pulse; i.e., they are alignment dependent. As a result, the rotational dynamics can be visualized by measuring the time-dependent yield of the dissociative-ionization channels [33,34], i.e., the D^+ ion yield, with the highest (lowest) yield expected when the molecules align parallel (perpendicular) to the probe polarization.

The laser pulses interacted not only with D_2 molecules inside He droplets but also with free D_2 molecules that diffused from the pickup cell to the target region. To eliminate

the background contribution from these isolated D_2 molecules and obtain a signal that exclusively originates from D_2 molecules embedded in the droplets, we recorded HeD^+ ions rather than D^+ ions. This strategy is similar to that employed in past studies on, e.g., I_2 molecules where HeI^+ ions were recorded [11,27]. The ultralow pressure ($\sim 10^{-7}$ mbar) in the interaction zone excluded the possibility that the fragment ion D^+ from a gas-phase isolated D_2 molecule collided with diffusing He atoms, required to form HeD^+ ions. The HeD^+ ions stem from, we believe, D^+ fragment ions binding to a He atom as they travel out of the droplet.

Figure 1(c) depicts the measured position y-TOF spectrum of the ions produced by the probe pulse. The spectrum consists of two series of singly charged ionic fragments with mass-to-charge ratio $m/q = 4n$ and $m/q = 4n + 2$ ($n = 1, 2, 3, 4, \ldots$), which are respectively assigned to He_n^+ and He_nD^+ ions [35]. The $m/q = 4n$ may also have a contribution from $He_{n-1}D_2^+$ ions. The signals with $1000 <$ TOF < 2000 ns are mainly from D^+ ions produced when D_2 molecules are dissociatively ionized. In what follows, we focus on the peak with $m/q = 6$ (marked by the dashed ellipse), which is assigned to HeD^+ ions and could only have originated from D_2 molecules embedded in helium droplets, as discussed above.

Figure 2(a) depicts the yield of the HeD^+ ions as a function of their kinetic energy (E_{kin}) and the time delay between the pump and the probe pulses. The time interval recorded was from -200 to 1000 fs with a step size of 6.7 fs. The E_{kin} axis is on a logarithmic scale, and the yield is normalized for each kinetic energy. Pronounced oscillation structures are visible with an apparent π-phase shift between ions with $0.1 < E_{\mathrm{kin}} < 1.0$ eV and ions with $E_{\mathrm{kin}} < 0.04$ eV. The yields integrated over the two E_{kin} ranges from 100 to 1000 fs are plotted in Fig. 2(b). The π-phase shift is evident, and it is seen that the two traces have the same oscillation period of $\sim$185 fs. Here, we focus on the high-E_{kin} fragments, i.e., HeD^+, and discuss the low E_{kin} in the Supplemental Material [18].

To explore the further evolution of the yield of the high-E_{kin} ions, measurements were conducted in the interval 1–7 ps with a step size of 10 fs. Figure 3(a) shows that the oscillations continue essentially without any change, a behavior qualitatively different from the alignment dynamics previously observed for I_2, CS_2, and OCS in He droplets [12]. The regular sine-like structure of the yield indicates that the D_2 rotational dynamics is the result of a wave packet dominated by two rotational quantum states [36]. To investigate if that is the case, the time-dependent HeD^+ yield from 1 to 7 ps was Fourier transformed. The power spectrum, represented by the red curve in Fig. 3(c), contains three peaks, of which the one centered at 5.35 THz is the dominant one.

Like past studies on both isolated and in-droplet molecules, one may expect that the central value of each spectral peak is given by the frequency of a $(J - J + 2)$ coherence

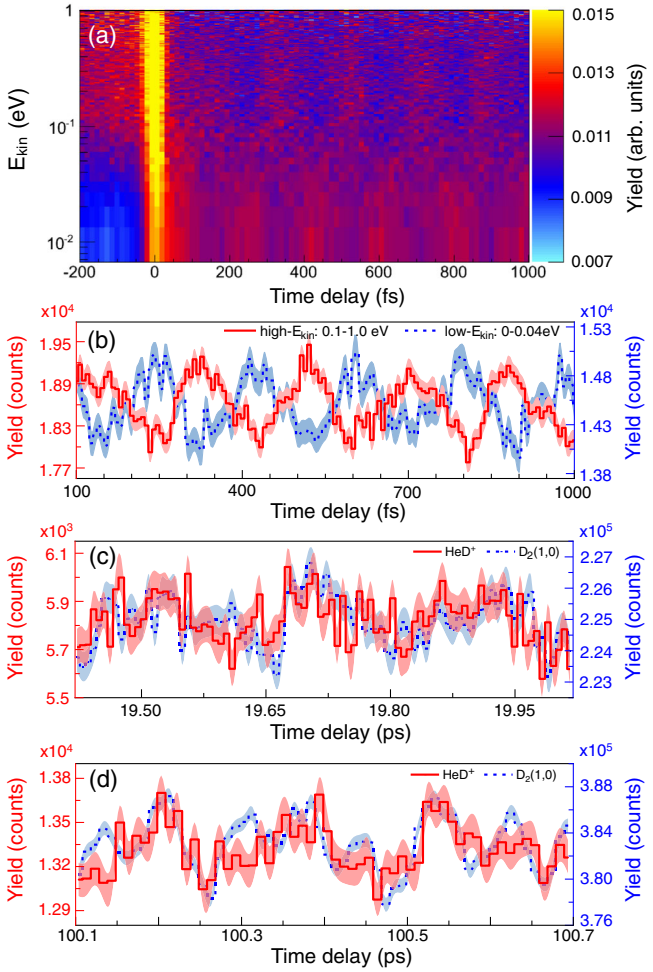

FIG. 2. (a) Yield of the ionic fragments with $m/q = 6$ as a function of the kinetic energy and the time delay. (b) Time-dependent yield obtained by integrating the yield over the low-E_{kin} and the high-E_{kin} ranges. (c),(d) Time-dependent yields of HeD^+ (from D_2 in He droplets) and D^+ [from the $D_2(1,0)$ channel of the isolated gas-phase D_2 molecules] in two selected time intervals. The shaded area represents the error bars. The time step sizes for the intervals of 19.42–20.02 and 100.1–100.7 ps are 6.7 and 10 fs, respectively.

in the rotational wave packets created by the alignment pulse, where J is the rotational angular momentum. Consequently, we assign the three observed peaks at 5.35, 8.92, and 12.40 THz as the (0–2), (1–3), and (2–4) coherences, respectively. The observation that the 5.35 THz peak is by far the strongest shows that this frequency dominates the rotational dynamics. This is consistent with the observed period of $\sim$185 fs in the time-dependent yield of HeD^+.

In Fig. 3(d), the central frequencies of the spectral peaks are plotted as a function of J. In analogy with previous studies, we fit the data points to $B(4J+6) - D(8J^3 + 36J^2 + 60J + 36)$, which is the expression for the frequencies of the $(J - J + 2)$ coherences for a nonrigid linear molecule, characterized by the rotational constant B and the centrifugal distortion

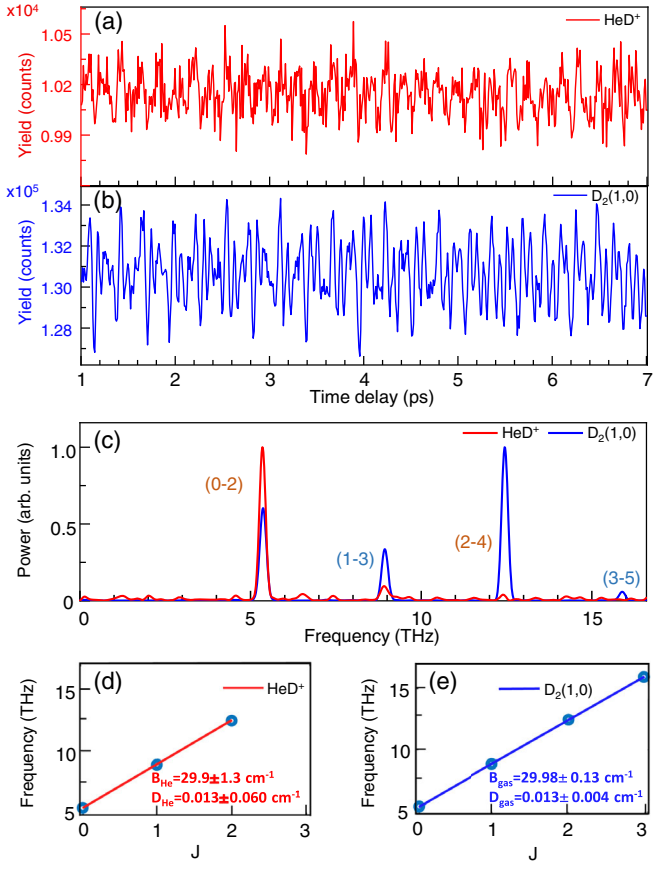

FIG. 3. (a),(b) Time-dependent yields of HeD^+ (from D_2 in He droplets) and D^+ [from the $D_2(1,0)$ channel of the gas-phase D_2 molecules] in the 1–7 ps time interval. (c) Power spectra of the yield traces in (a) and (b). (d),(e) Central frequencies of $(J - J + 2)$ peaks in the power spectra versus J. The full lines represent the best fits using the least square method; see text. The B and D constants from the fits are given with 95% confidence bounds.

constant D [12]. The best fit, shown by the red curve in Fig. 3(d), is obtained for $B_{\mathrm{He}} = 29.9 \pm 1.3\ \mathrm{cm}^{-1}$ and $D_{\mathrm{He}} = 0.013 \pm 0.060\ \mathrm{cm}^{-1}$, with units converted from THz to cm^{-1} (see the discussion on uncertainty in Ref. [18], Sec. III). There is a large relative uncertainty on both B_{He} and D_{He} because the fit is based only on three points. In particular, for D_{He}, the uncertainty is larger than the central value but the result still shows that $D_{\mathrm{He}} \ll B_{\mathrm{He}}$ and allows us to conclude that the $D_{\mathrm{He}} = 0.038 B_{\mathrm{He}}^{1.88}$ correlation [15] indeed does not apply to D_2 molecules, similar to the case of methane molecules in helium droplets [17]. Moreover, using the reported formula obtained within a simplified angulon model [13], we estimate $D_{\mathrm{He}} = 0.001\ \mathrm{cm}^{-1}$ for D_2 (see Ref. [18], Sec. V), which lies within the uncertainty range. Our results are the first measured values of B_{He} and D_{He} for D_2 molecules embedded in He droplets.

As a reference, the time-dependent yield for isolated D_2 molecules in the background, measured using D^+ as the observable [blue curve in Fig. 3(b)], exhibits an oscillatory structure similar to that of the HeD^+ signal in Fig. 3(a). The corresponding power spectrum, shown by the blue curve in Fig. 3(c), contains four peaks which we assign as the (0–2), (1–3), (2–4), and (3–5) coherences, respectively. The central positions of the spectral peaks, of which the first three essentially coincide with those for the D_2 molecules in He droplets, are plotted as a function of J in Fig. 3(e). Again, the experimental data points are fitted to the nonrigid rotor expression, and we find that the best fit, represented by the blue curve, is obtained for $B_{\mathrm{gas}} = 29.98 \pm 0.13\ \mathrm{cm}^{-1}$, $D_{\mathrm{gas}} = 0.013 \pm 0.004\ \mathrm{cm}^{-1}$. Within the uncertainty of the experiment, these results are consistent with the values 29.91 and 0.01123 cm^{-1} obtained from either spectroscopic measurements or theoretical calculations [37–39].

Figure 3(c) shows that the relative intensities of the spectral peaks are not the same for the isolated and the in-droplet D_2 molecules. As we now explain, this is ascribed to a difference in the initial population $P(J)$ of the rotational states. For the isolated D_2 molecules, $P(J)$ is determined by a Boltzmann distribution with a rotational temperature T_{rot} equal to 295 K and taking into account the 2:1 nuclear spin statistical factor for the even (*ortho*-D_2) and odd (*para*-D_2) states: $P(0) = 19\%$, $P(1) = 21\%$, $P(2) = 39\%$, $P(3) = 11\%$, $P(4) = 9\%$, and $P(5) = 1\%$. With this population distribution, the parameters of the experimental alignment pulse, and the B_{gas} and D_{gas} values from the fit of the experimental data, we calculated $\langle \cos^2\theta \rangle(t)$, the standard metric for the degree of alignment, by solving the time-dependent rotational Schrödinger equation; here, θ is the angle between the alignment pulse polarization and the D_2 internuclear axis. Subsequently, Fourier transforming $\langle \cos^2\theta \rangle(t)$ gives a spectrum that is very close to the blue curve in Fig. 3(c) (see Ref. [18], Sec. IV). If $P(J)$ for the in-droplet D_2 molecules is determined by a Boltzmann distribution with $T_{\mathrm{rot}} = 0.37$ K as observed for molecules like SF_6 [40], OCS [41], CS_2, and I_2 [27], then only the $J = 0$ state should be populated. Only spectral peaks from coherences between states with even J values would be seen after the (cascade) Raman excitation by the alignment pulse. The observation of the (1–3) peak in Fig. 3(c) shows that some of the D_2 molecules inside the droplets are initially populated in states with odd J. Consequently, the time it takes a He droplet to fly from the pickup cell, where the D_2 molecules are embedded, to the interaction region with the laser beam, about 2.2 ms in our experiment, is not sufficient to completely thermalize the rotational state distribution initially at 295 K to one at 0.37 K. We believe this is due to the well-known long timescales for flipping the nuclear spin of the deuterons [42–44].

The information from the time-dependent HeD^+ yield and the corresponding power spectrum allows us to conclude that the laser-induced rotational dynamics of the D_2 molecules inside He droplets is determined mainly by the (0–2) coherence with frequency 5.35 THz.

The unchanged amplitude of HeD^+ in the 1–7 ps interval shows that inhomogeneous and homogeneous broadenings are negligible on this timescale. To explore dynamics on longer timescales, data were recorded in the intervals 19.42–20.02 ps and 100.1–100.7 ps; see Figs. 2(c)–(d). Because of the significant acquisition times required, measurements were restricted to these two selected time windows. Again, the D^+ signal from isolated molecules was recorded as a reference. The signals measured in both time intervals demonstrate that the 185-fs oscillations are still present, even after 100 ps, although with a somewhat reduced amplitude compared to the first 7 ps. These observations show that the dominant (0–2) coherence of the rotational wave packet is preserved for more than 500 oscillations and that the $J = 2$ state has a lifetime of at least 100 ps. This is in accordance with a recent theoretical study investigating the influence of the rotational constants, the initial rotational state, and the droplet size on rotational relaxation dynamics of fast rotors inside helium nanodroplets [45]. The calculations predicted that rotational relaxation of D_2 ($J = 2$, $M_J = 0$) in superfluid helium nanodroplets could be >5 ns due to the weak molecule-helium interaction. Consistent with this, we suggest that the low density of states of superfluid helium [46,47] at the energies of the excited rotational states of D_2 is responsible for the weak coupling of the molecular rotation with the helium excitations. Also, we note that the energies of the excited rotational states are significantly larger than the He-D_2 binding energy. Thus, creating a coherent superposition of $J = 0$ and 2 would be enough to decouple the molecule from the surrounding helium [11,48], in line with the classical picture of a light rotor carving out a cavity in which it rotates [15].

In summary, we experimentally investigated laser-induced field-free molecular alignment dynamics of D_2 molecules inside He droplets. The dominant (0–2) rotational coherence has an energy (179 cm^{-1}) much above the roton energy of the droplets and persists for longer than 100 ps. From the power spectra of the alignment traces, B_{He} was determined and found to be the same as B_{gas}. In total, our measurements show that for at least 100 ps, equivalent to >500 rotational periods, D_2 molecules in He droplets rotate as if they were isolated gas-phase particles. This behavior is strikingly different from the in-droplet rotation of all other molecules studied [49]. It would be interesting to investigate the rotational dynamics for significantly longer times to find out when coupling between the D_2 rotation and the droplet becomes important. This is in principle possible with our technique. So are studies on other light molecules like HF and C_2H_2, which would explore the rotational dynamics of rotors in the gap between the superlight D_2 and the heavier species like OCS.

This work is supported by the National Key R&D Program of China (Grant No. 2018YFA0306303); the National Natural Science Fund (Grants No. 11834004, No. 11621404, and No. 12174109); the project supported by the Shanghai Committee of Science and Technology (Grant No. 19JC1412200). J. Q. acknowledges support by ECNU Cultivation Project of Future Scientist & Outstanding Scholar (Grant No. WLKXJ202003). H. S. acknowledges support from the Villum Foundation through a Villum Investigator Grant No. 25886. M. L. acknowledges support by the European Research Council (ERC) Starting Grant No. 801770 (ANGULON). I. N. C. acknowledges support by the European Union's Horizon 2020 research and innovation programme under the Marie Sklodowska-Curie Grant Agreement No. 665385.

*These authors contributed equally to this work.
†pflu@lps.ecnu.edu.cn
‡henriks@chem.au.dk
§jwu@phy.ecnu.edu.cn

[1] H. Stapelfeldt and T. Seideman, Colloquium: Aligning molecules with strong laser pulses, Rev. Mod. Phys. **75**, 543 (2003).
[2] C. P. Koch, M. Lemeshko, and D. Sugny, Quantum control of molecular rotation, Rev. Mod. Phys. **91**, 035005 (2019).
[3] S. Fleischer, Y. Khodorkovsky, E. Gershnabel, Y. Prior, and I. Sh. Averbukh, Molecular alignment induced by ultrashort laser pulses and its impact on molecular motion, Isr. J. Chem. **52**, 414 (2012).
[4] Y. Ohshima and H. Hasegawa, Coherent rotational excitation by intense nonresonant laser fields, Int. Rev. Phys. Chem. **29**, 619 (2010).
[5] E. F. Thomas, A. A. Søndergaard, B. Shepperson, N. E. Henriksen, and H. Stapelfeldt, Hyperfine-Structure-Induced Depolarization of Impulsively Aligned I_2 Molecules, Phys. Rev. Lett. **120**, 163202 (2018).
[6] L. V. Thesing, A. Yachmenev, R. González-Férez, and J. Küpper, The effect of nuclear-quadrupole coupling in the laser-induced alignment of molecules, J. Phys. Chem. A **124**, 2225 (2020).
[7] J. Ma, H. Zhang, B. Lavorel, F. Billard, E. Hertz, J. Wu, C. Boulet, J.-M. Hartmann, and O. Faucher, Observing collisions beyond the secular approximation limit, Nat. Commun. **10**, 5780 (2019).
[8] T. Vieillard, F. Chaussard, D. Sugny, B. Lavorel, and O. Faucher, Field-free molecular alignment of CO_2 mixtures in presence of collisional relaxation, J. Raman Spectrosc. **39**, 694 (2008).
[9] N. Owschimikow, F. Königsmann, J. Maurer, P. Giese, A. Ott, B. Schmidt, and N. Schwentner, Cross sections for rotational decoherence of perturbed nitrogen measured via decay of laser-induced alignment, J. Chem. Phys. **133**, 044311 (2010).
[10] D. Pentlehner, J. H. Nielsen, A. Slenczka, K. Mølmer, and H. Stapelfeldt, Impulsive Laser Induced Alignment of Molecules Dissolved in Helium Nanodroplets, Phys. Rev. Lett. **110**, 093002 (2013).
[11] B. Shepperson, A. A. Søndergaard, L. Christiansen, J. Kaczmarczyk, R. E. Zillich, M. Lemeshko, and H. Stapelfeldt, Laser-Induced Rotation of Iodine Molecules

in Helium Nanodroplets: Revivals and Breaking Free, Phys. Rev. Lett. **118**, 203203 (2017).
[12] A. S. Chatterley, L. Christiansen, C. A. Schouder, A. V. Jørgensen, B. Shepperson, I. N. Cherepanov, G. Bighin, R. E. Zillich, M. Lemeshko, and H. Stapelfeldt, Rotational Coherence Spectroscopy of Molecules in Helium Nanodroplets: Reconciling the Time and the Frequency Domains, Phys. Rev. Lett. **125**, 013001 (2020).
[13] I. N. Cherepanov, G. Bighin, C. A. Schouder, A. S. Chatterley, S. H. Albrechtsen, A. V. Muñoz, L. Christiansen, H. Stapelfeldt, and M. Lemeshko, Excited rotational states of molecules in a superfluid, Phys. Rev. A **104**, L061303 (2021).
[14] J. P. Toennies and A. F. Vilesov, Superfluid helium droplets: A uniquely cold nanomatrix for molecules and molecular complexes, Angew. Chem., Int. Ed. **43**, 2622 (2004).
[15] M. Y. Choi, G. E. Douberly, T. M. Falconer, W. K. Lewis, C. M. Lindsay, J. M. Merritt, P. L. Stiles, and R. E. Miller, Infrared spectroscopy of helium nanodroplets: Novel methods for physics and chemistry, Int. Rev. Phys. Chem. **25**, 15 (2006).
[16] Y. Kwon, P. Huang, M. V. Patel, D. Blume, and K. B. Whaley, Quantum solvation and molecular rotations in superfluid helium clusters, J. Chem. Phys. **113**, 6469 (2000).
[17] K. Nauta and R. E. Miller, Rotational and vibrational dynamics of methane in helium nanodroplets, Chem. Phys. Lett. **350**, 225 (2001).
[18] See Supplemental Material at http://link.aps.org/supplemental/10.1103/PhysRevLett.128.243201, which includes Refs. [19–23], for details on experimental methods, analysis and calculations.
[19] A. Braun and M. Drabbels, Photodissociation of alkyl iodides in helium nanodroplets. I. Kinetic energy transfer, J. Chem. Phys. **127**, 114303 (2007).
[20] A. Khan, T. Jahnke, S. Zeller, F. Trinter, M. Schöffler, L. Ph. H. Schmidt, R. Dörner, and M. Kunitski, Visualizing the geometry of hydrogen dimers, J. Phys. Chem. Lett. **11**, 2457 (2020).
[21] I. N. Cherepanov, G. Bighin, C. A. Schouder, A. S. Chatterley, H. Stapelfeldt, and M. Lemeshko, A simple model for high rotational excitations of molecules in a superfluid, arXiv:2201.13030.
[22] F. M. Tao, An accurate ab initio potential energy surface of the $He-H_2$ interaction, J. Chem. Phys. **100**, 4947 (1994).
[23] M. Lemeshko, Quasiparticle Approach to Molecules Interacting with Quantum Solvents, Phys. Rev. Lett. **118**, 095301 (2017).
[24] R. Dörner, V. Mergel, O. Jagutzki, L. Spielberger, J. Ullrich, R. Moshammer, and H. Schmidt-Böcking, Cold target recoil ion momentum spectroscopy: A 'momentum microscope' to view atomic collision dynamics, Phys. Rep. **330**, 95 (2000).
[25] J. Ullrich, R. Moshammer, R. Dorn, R. Dörner, L. Ph. H. Schmidt, and H. Schmidt-Böcking, Recoil-ion and electron momentum spectroscopy: Reaction-microscopes, Rep. Prog. Phys. **66**, 1463 (2003).
[26] T. E. Sharp, Potential-energy curves for molecular hydrogen and its ions, At. Data Nucl. Data Tables **2**, 119 (1970).
[27] B. Shepperson, A. S. Chatterley, A. A. Søndergaard, L. Christiansen, M. Lemeshko, and H. Stapelfeldt, Strongly aligned molecules inside helium droplets in the near-adiabatic regime, J. Chem. Phys. **147**, 013946 (2017).
[28] A. S. Chatterley, C. Schouder, L. Christiansen, B. Shepperson, M. H. Rasmussen, and H. Stapelfeldt, Long-lasting field-free alignment of large molecules inside helium nanodroplets, Nat. Commun. **10**, 133 (2019).
[29] A. Staudte, S. Patchkovskii, D. Pavičić, H. Akagi, O. Smirnova, D. Zeidler, M. Meckel, D. M. Villeneuve, R. Dörner, M. Y. Ivanov, and P. B. Corkum, Angular Tunneling Ionization Probability of Fixed-in-Space H_2 Molecules in Intense Laser Pulses, Phys. Rev. Lett. **102**, 033004 (2009).
[30] S. F. Zhao, C. Jin, A.-T. Le, T. F. Jiang, and C. D. Lin, Determination of structure parameters in strong-field tunneling ionization theory of molecules, Phys. Rev. A **81**, 033423 (2010).
[31] P. H. Bucksbaum, A. Zavriyev, H. G. Muller, and D. W. Schumacher, Softening of the H_2^+ Molecular Bond in Intense Laser Fields, Phys. Rev. Lett. **64**, 1883 (1990).
[32] T. Zuo and A. D. Bandrauk, Charge-resonance-enhanced ionization of diatomic molecular ions by intense lasers, Phys. Rev. A **52**, R2511 (1995).
[33] Y. Mi, P. Peng, N. Camus, X. Sun, P. Fross, D. Martinez, Z. Dube, P. B. Corkum, D. M. Villeneuve, A. Staudte, R. Moshammer, and T. Pfeifer, Clocking Enhanced Ionization of Hydrogen Molecules with Rotational Wave Packets, Phys. Rev. Lett. **125**, 173201 (2020).
[34] J. Mikosch, C. Z. Bisgaard, A. E. Boguslavskiy, I. Wilkinson, and A. Stolow, The quantitative determination of laser-induced molecular axis alignment, J. Chem. Phys. **139**, 024304 (2013).
[35] M. Fárník and J. P. Toennies, Ion-molecule reactions in ^{4}He droplets: Flying nano-cryo-reactors, J. Chem. Phys. **122**, 014307 (2005).
[36] A. Przystawik, A. Kickermann, A. Al-Shemmary, S. Düsterer, A. M. Ellis, K. von Haeften, M. Harmand, S. Ramakrishna, H. Redlin, L. Schroedter, M. Schulz, T. Seideman, N. Stojanovic, J. Szekely, F. Tavella, S. Toleikis, and T. Laarmann, Generation of the simplest rotational wave packet in a diatomic molecule: Tracing a two-level superposition in the time domain, Phys. Rev. A **85**, 052503 (2012).
[37] J. Komasa, K. Piszczatowski, G. Łach, M. Przybytek, B. Jeziorski, and K. Pachucki, Quantum electrodynamics effects in rovibrational spectra of molecular hydrogen, J. Chem. Theory Comput. **7**, 3105 (2011).
[38] A. de Lange, G. D. Dickenson, E. J. Salumbides, W. Ubachs, N. de Oliveira, D. Joyeux, and L. Nahon, VUV Fourier-transform absorption study of the Lyman and Werner bands in D_2, J. Chem. Phys. **136**, 234310 (2012).
[39] D. E. Jennings, A. Weber, and J. W. Brault, Raman spectroscopy of gases with a Fourier transform spectrometer: The spectrum of D_2, Appl. Opt. **25**, 284 (1986).
[40] M. Hartmann, R. E. Miller, J. P. Toennies, and A. Vilesov, Rotationally Resolved Spectroscopy of SF_6 in Liquid Helium Clusters: A Molecular Probe of Cluster Temperature, Phys. Rev. Lett. **75**, 1566 (1995).
[41] S. Grebenev, M. Hartmann, M. Havenith, B. Sartakov, J. P. Toennies, and A. F. Vilesov, The rotational spectrum of

single OCS molecules in liquid ^{4}He droplets, J. Chem. Phys. **112**, 4485 (2000).
[42] I. F. Silvera, The solid molecular hydrogens in the condensed phase: Fundamentals and static properties, Rev. Mod. Phys. **52**, 393 (1980).
[43] Y. Y. Milenko, R. M. Sibileva, and M. A. Strzhemechny, Natural ortho-para conversion rate in liquid and gaseous hydrogen, J. Low Temp. Phys. **107**, 77 (1997).
[44] K. Urano and K. Motizuki, Ortho-para conversion of H_2 and D_2 diluted in solid HD, Solid State Commun. **5**, 691 (1967).
[45] M. Blancafort-Jorquera, A. Vilà, and M. González, Rotational energy relaxation quantum dynamics of a diatomic molecule in a superfluid helium nanodroplet and study of the hydrogen isotopes case, Phys. Chem. Chem. Phys. **21**, 21007 (2019).
[46] M. Hartmann, F. Mielke, J. P. Toennies, A. F. Vilesov, and G. Benedek, Direct Spectroscopic Observation of Elementary Excitations in Superfluid He Droplets, Phys. Rev. Lett. **76**, 4560 (1996).
[47] K. Nauta and R. E. Miller, The vibrational and rotational dynamics of acetylene solvated in superfluid helium nanodroplets, J. Chem. Phys. **115**, 8384 (2001).
[48] P. Vindel-Zandbergen, J. Jiang, M. Lewerenz, C. Meier, M. Barranco, M. Pi, and N. Halberstadt, Impulsive alignment of $^4He - CH_3I$: A theoretical study, J. Chem. Phys. **149**, 124301 (2018).
[49] Perhaps with the exception of the HF molecule (Ref. [50]).
[50] K. Nauta and R. E. Miller, Metastable vibrationally excited HF ($v = 1$) in helium nanodroplets, J. Chem. Phys. **113**, 9466 (2000).